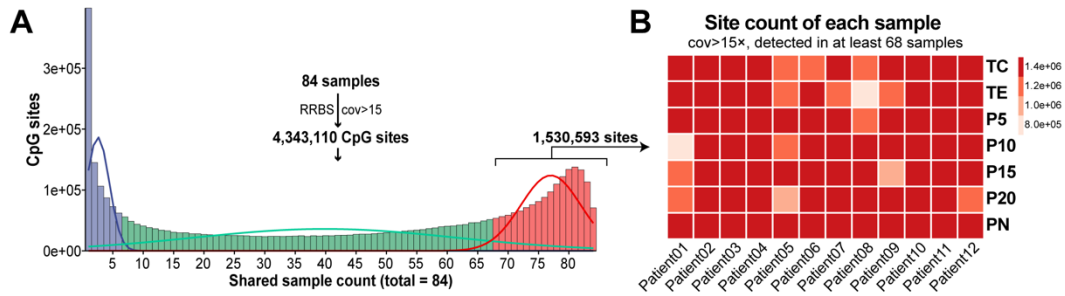


APPENDIX

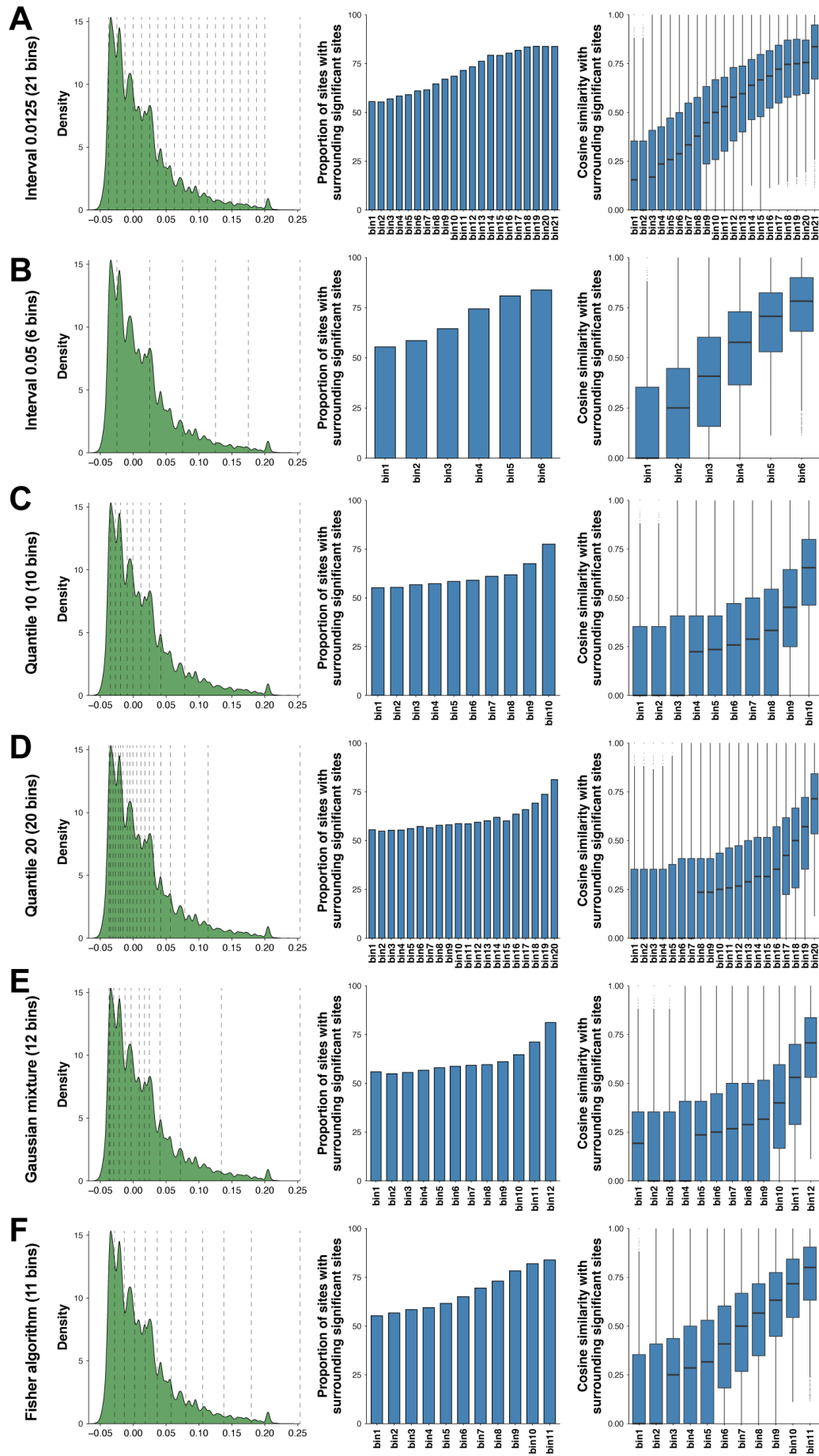
Table of Contents

Appendix Figure S1	2
Appendix Figure S2	4
Appendix Figure S3	5
Appendix Figure S4	7
Appendix Figure S5	9
Appendix Figure S6	11
Appendix Figure S7	13
Appendix Figure S8	14
Appendix Figure S9	15
Appendix Figure S10	17
Appendix Methods.....	18



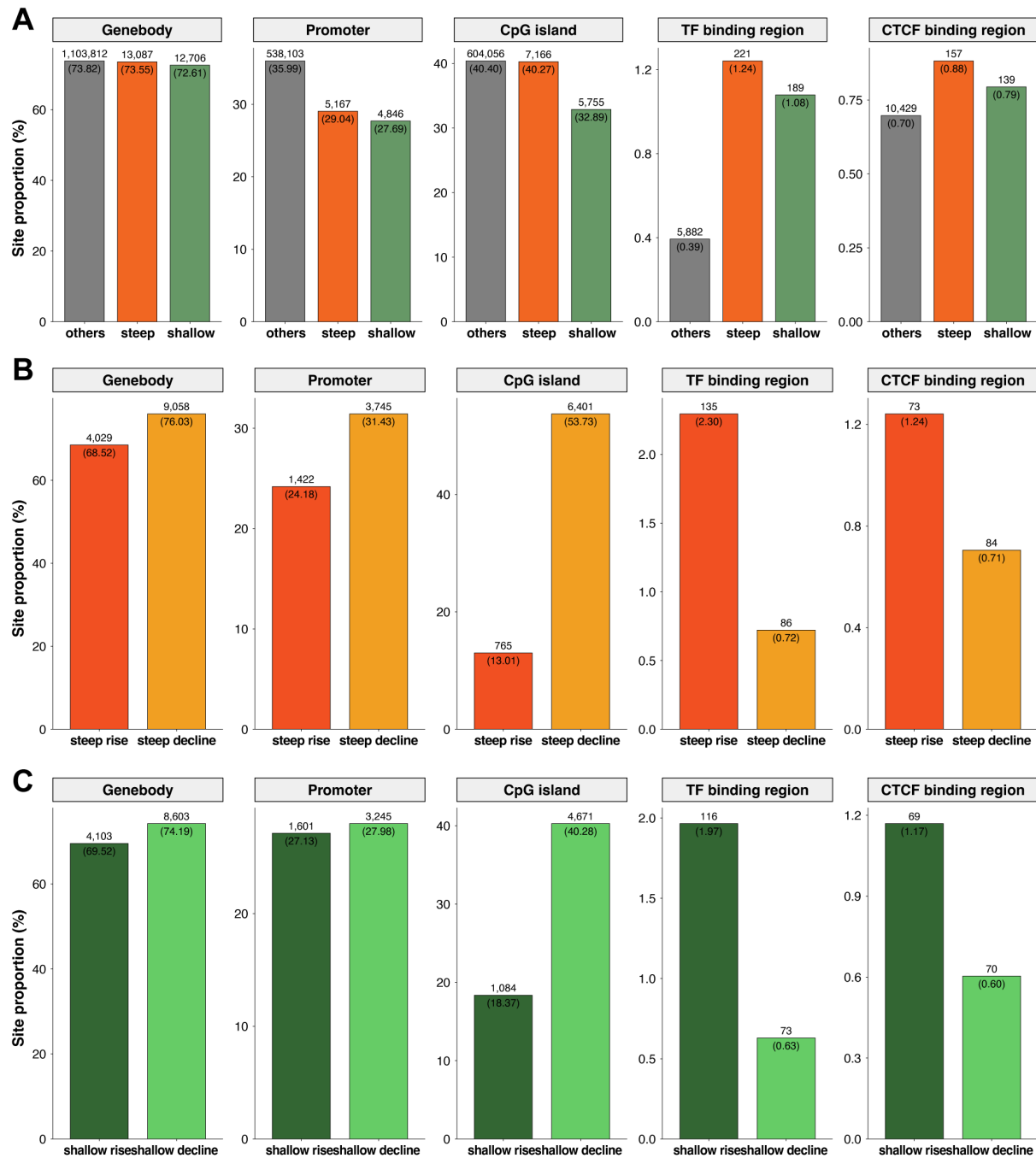
Appendix Figure S1. RRBS quality control and count of CpG sites in each sample.

(A) Frequency distribution of all detected CpG sites ($n = 4,343,110$) is presented. The threshold was determined at 68 based on the Gaussian mixture model analysis, which revealed three distributions at their intersection points. Consequently, 1,530,593 sites were retained for further analysis. **(B)** The number of detected CpG sites in each sample among the retained 1,530,593 CpG sites is illustrated.



Appendix Figure S2. Robustness of the association between Moran's *I* and spatial ordering of sites across different binning strategies.

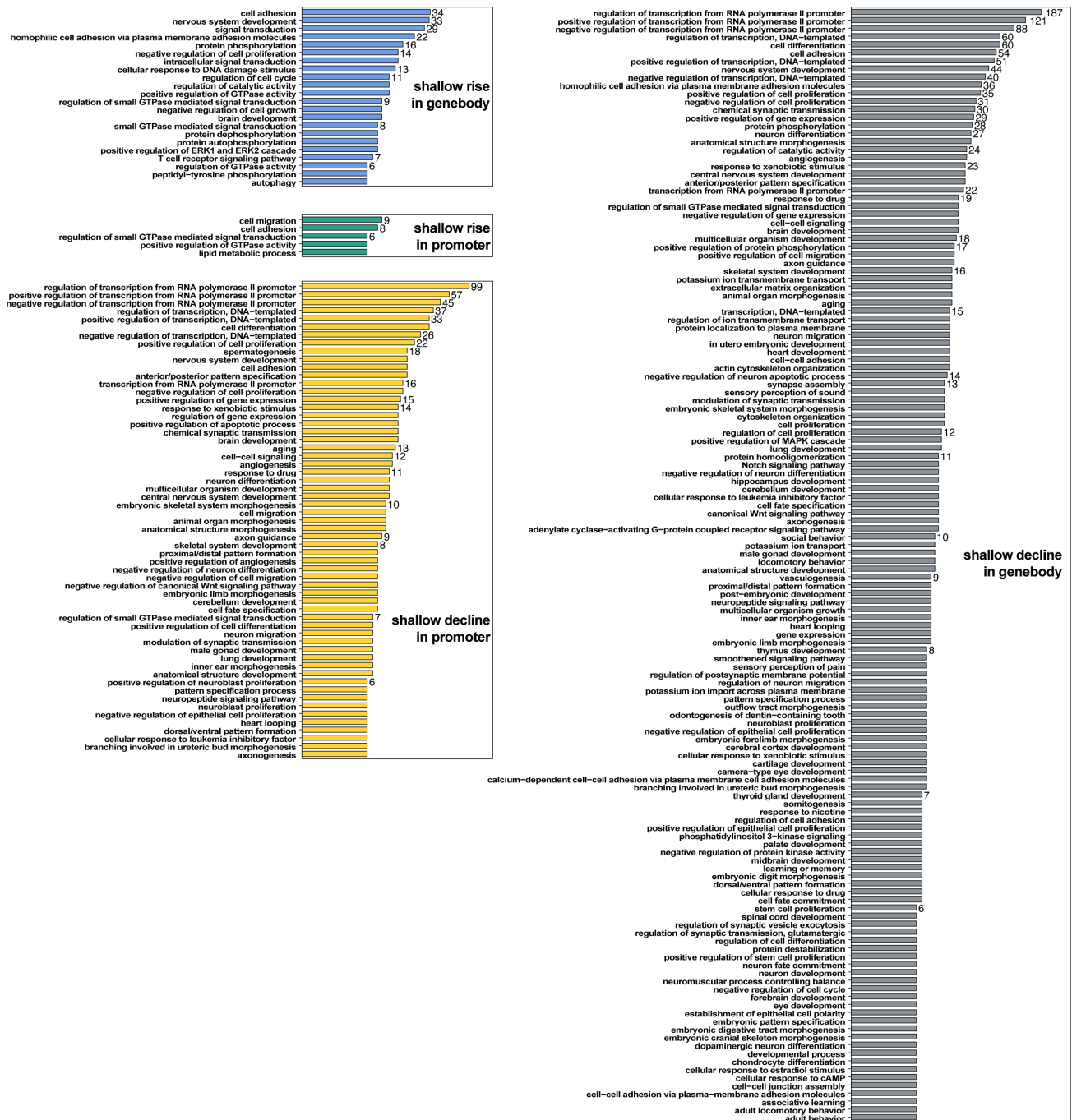
To evaluate the robustness of the observed correlation between Moran's *I* and spatial ordering of CpG sites, six binning strategies were applied: **(A)** fixed-width bins at 0.0125 intervals (21 bins), **(B)** fixed-width bins at 0.05 intervals (6 bins), **(C)** equal-sized quantile bins (10 bins), **(D)** quantile-based bins with finer resolution (20 bins), **(E)** bins generated by Gaussian mixture model (GMM) using the expectation-maximization (EM) algorithm (12 bins), and **(F)** bins defined by Fisher-Jenks natural breaks optimization (11 bins). For each strategy, we calculated the proportion of sites with at least one differentially methylated neighbor within ± 30 nucleotides (middle panels) and the cosine similarity between each site and its neighbors (right panels). Across all binning methods, both metrics consistently increased with Moran's *I*, supporting the robustness of the observed ordering pattern. Detailed computational procedures and representative examples are provided in Fig. EV2.



Appendix Figure S3. Genomic context distribution of CpG sites with steep and shallow methylation changes.

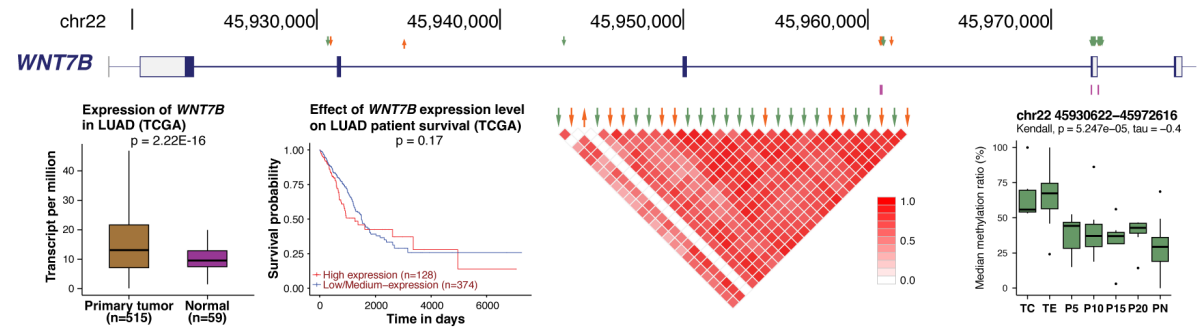
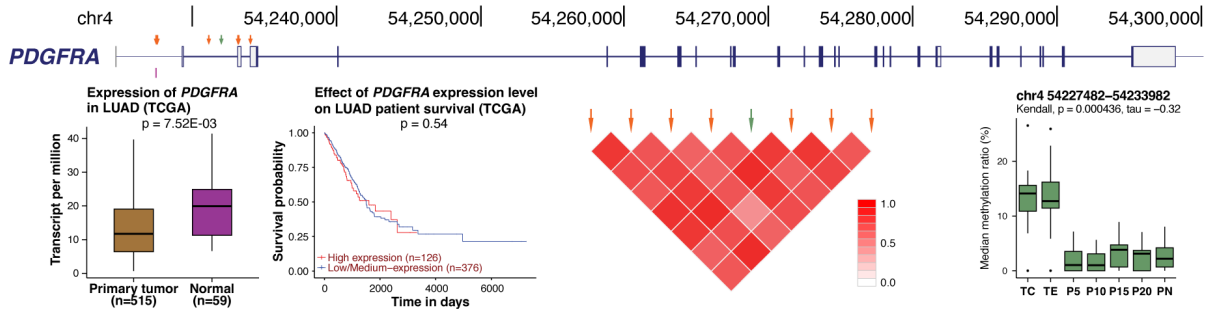
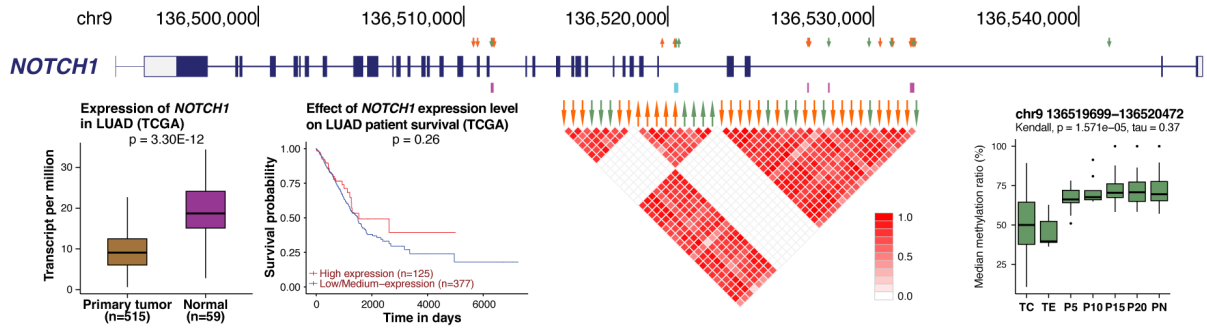
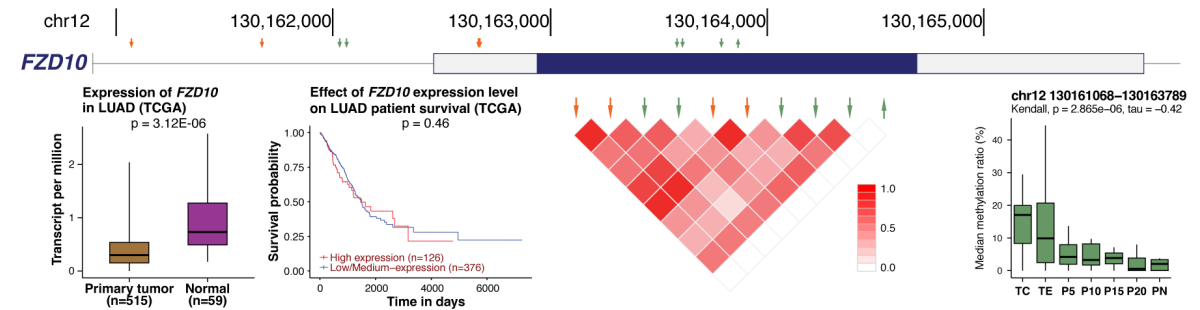
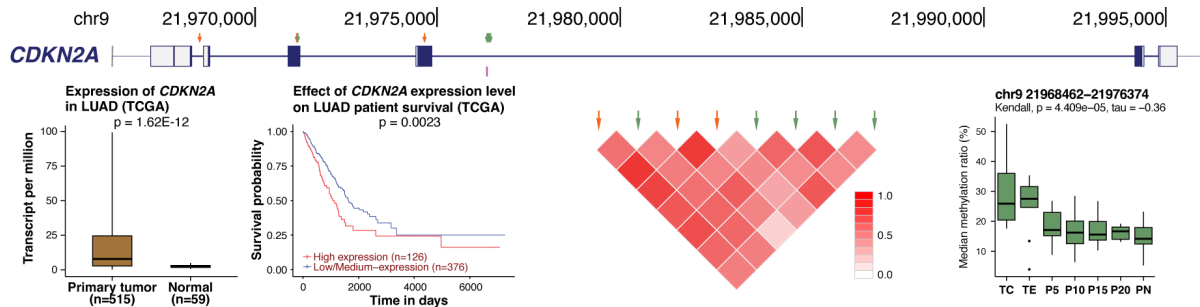
(A) Comparison of CpG sites with steep ($n = 17,794$, orange) and shallow ($n = 17,498$, green) methylation changes against all other detected CpG sites ($n = 1,495,301$, grey) across five genomic

features: gene bodies, promoters (2 kb upstream of TSS), CpG islands, transcription factor (TF) binding regions, and CTCF binding regions. **(B)** Feature distribution of steep rise and steep decline sites. **(C)** Feature distribution of shallow rise and shallow decline sites. Site counts and their corresponding proportions are labeled on each bar.



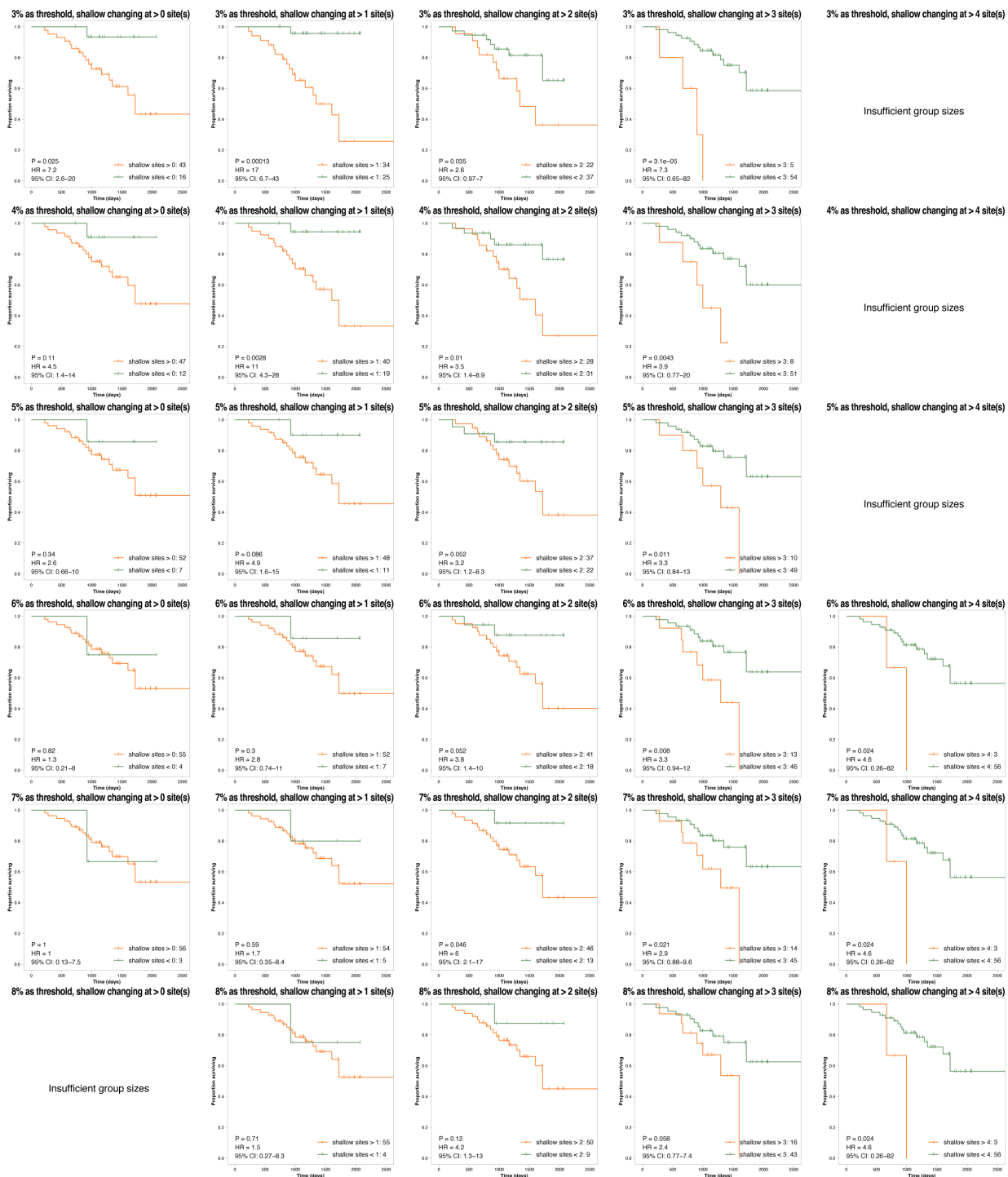
Appendix Figure S4. GO analysis of genes associated with methylation-changing regions.

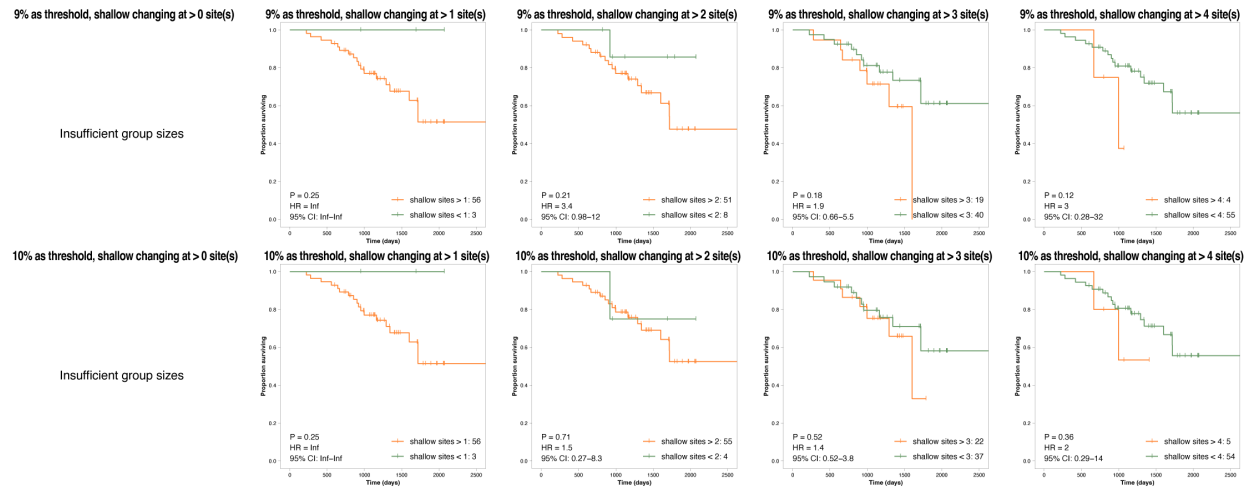
GO analysis was conducted on genes containing only shallow- or mixed-changing regions, with a filter applied for gene count > 5 and P-value < 0.05. Bars represent relative gene counts. Genes with multiple changing regions were included only once per analysis for each changing type.



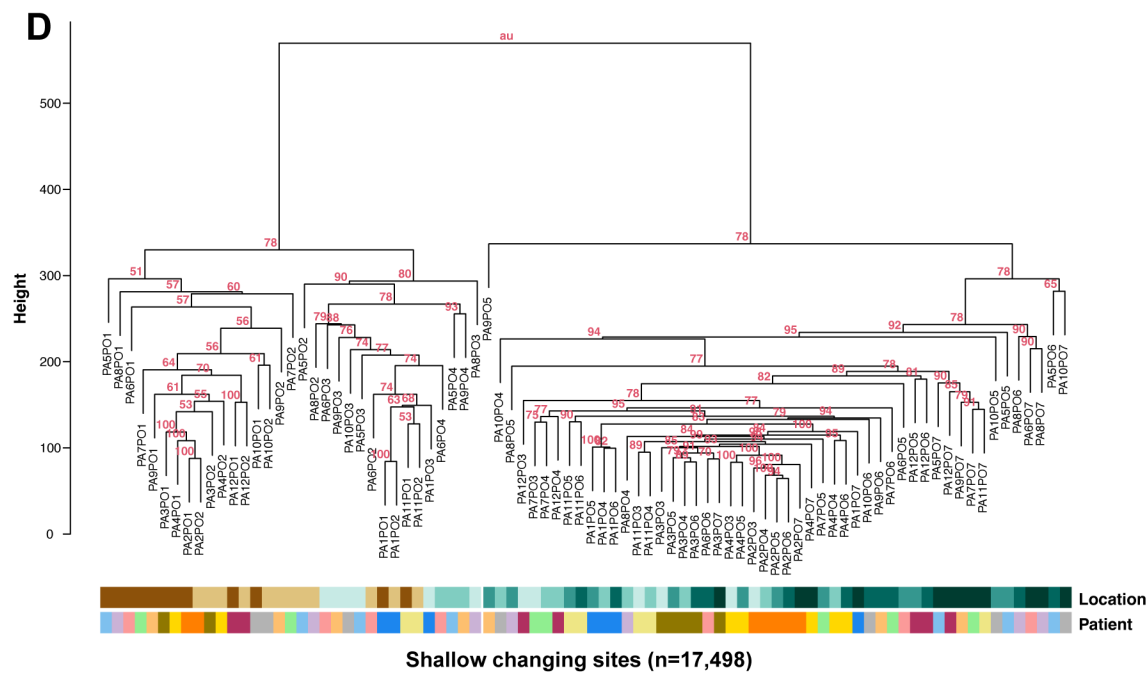
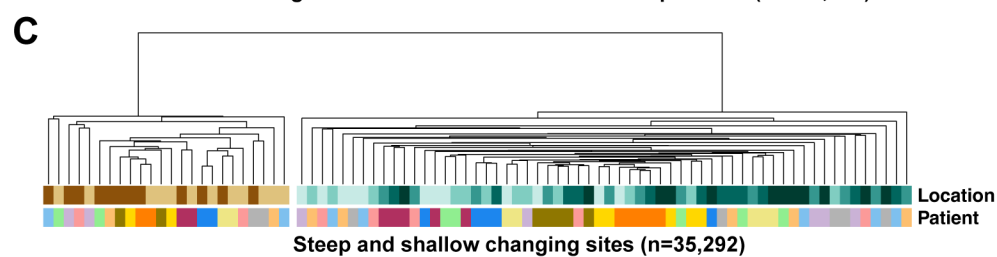
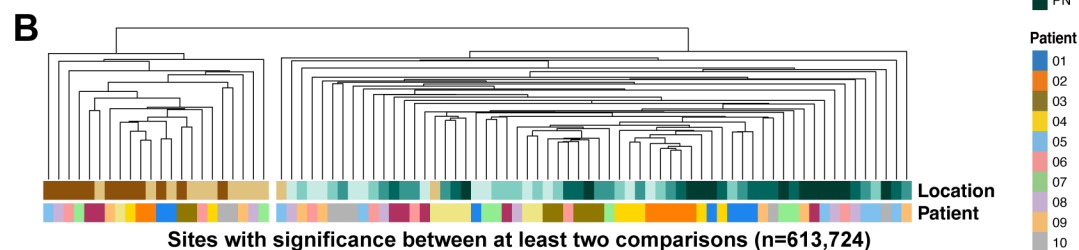
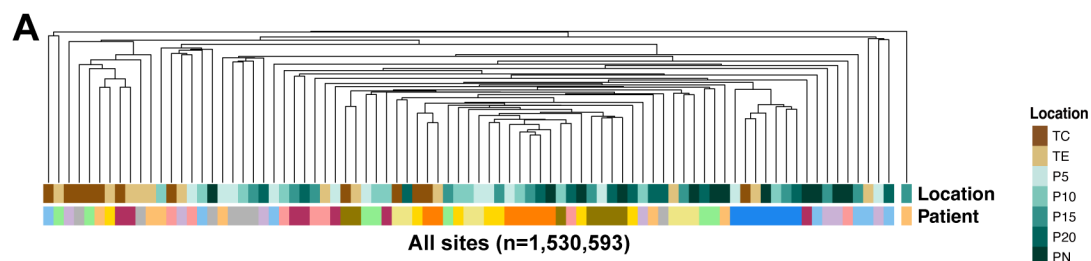
Appendix Figure S5. Methylation-changing CpG sites and transcriptional features of five target genes.

Genomic distributions of methylation-changing CpG sites are shown first. Gene expression levels of the five genes in primary LUAD and normal tissues based on TCGA data. Kaplan–Meier survival curves of TCGA-LUAD patients stratified by expression levels of each gene. Cosine similarity of CpG sites on each gene. Median methylation levels across seven spatially resolved tissue locations (TC, TE, P5, P10, P15, P20, PN) for each gene, were calculated from CpG sites located in genebody and promoter regions.



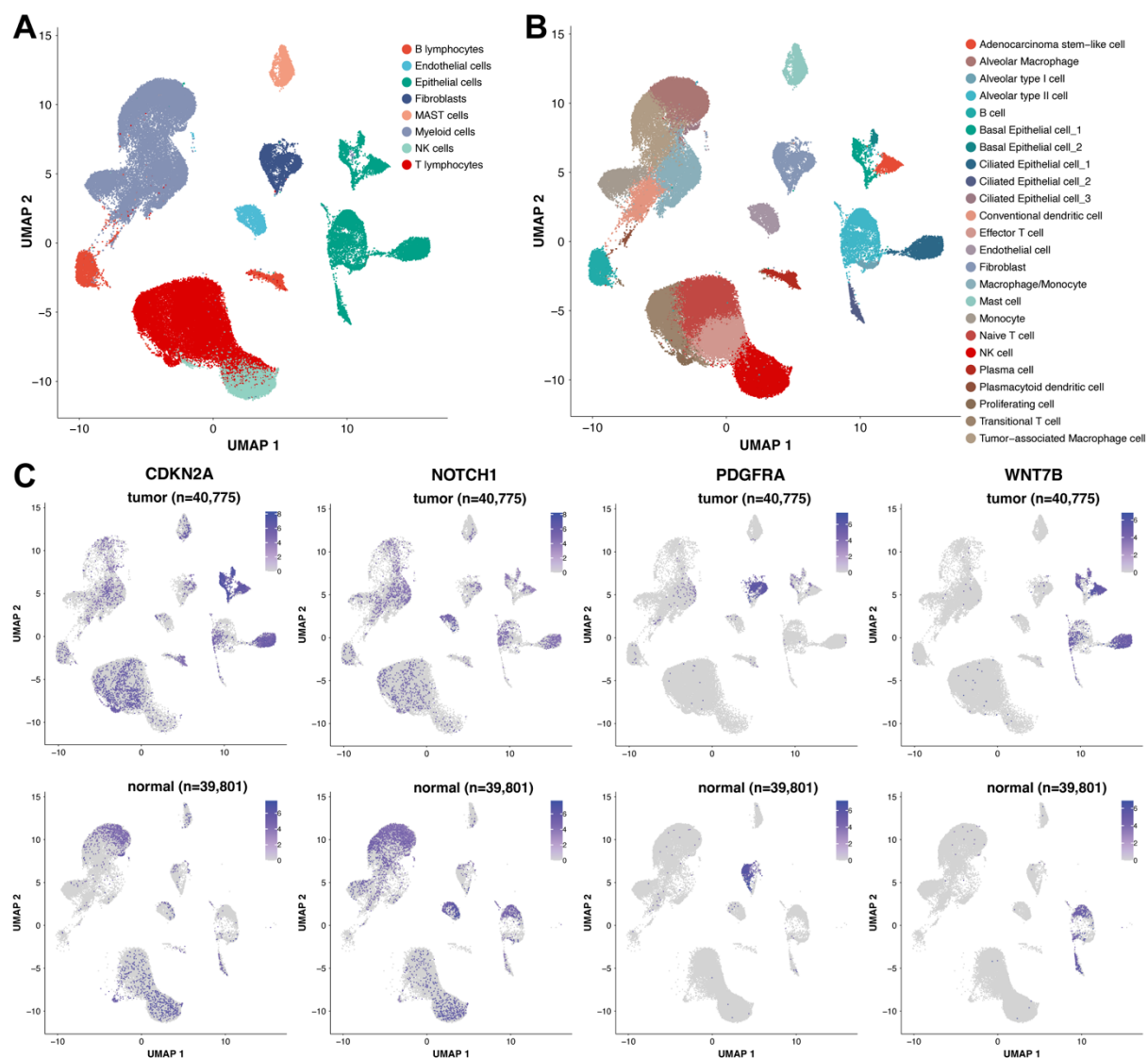


Appendix Figure S6. Kaplan-Meier survival analysis for patients based on the number of sites with shallow DNA methylation changes.



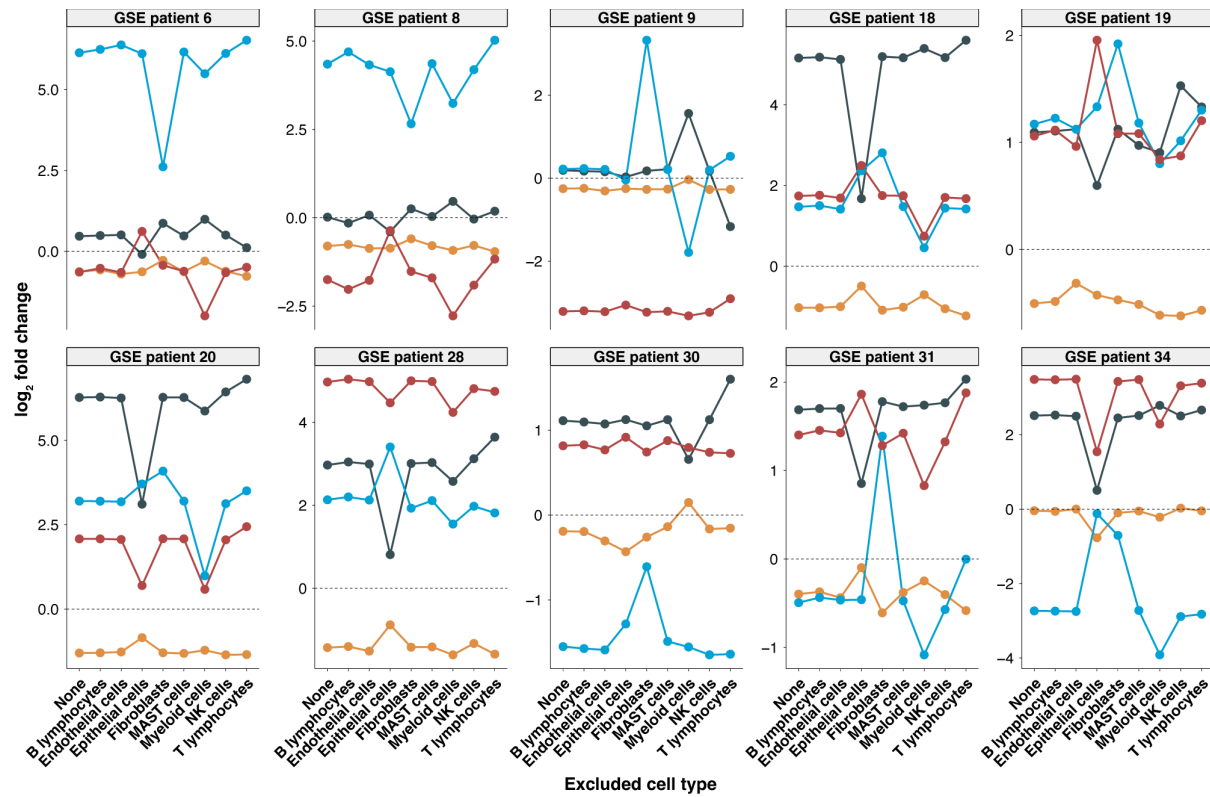
Appendix Figure S7. Hierarchical clustering based on different sets of CpG sites.

(A) Clustering of samples using all ~1.53 million CpG sites did not reveal distinct tumor-normal separation. (B) Clustering based on ~610,000 filtered CpGs (with ≥ 2 significant differences) showed clearer tumor grouping, though two TE samples clustered with adjacent tissues. (C) Clustering using the combined set of steep and shallow changing CpG sites ($n = 35,292$). (D) Cluster stability was assessed using pvcust with multiscale bootstrap resampling; high AU values support the clustering of some adjacent samples (P5/P10) with tumor samples.



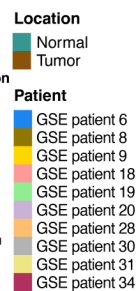
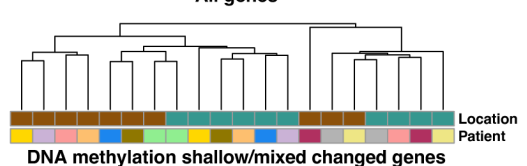
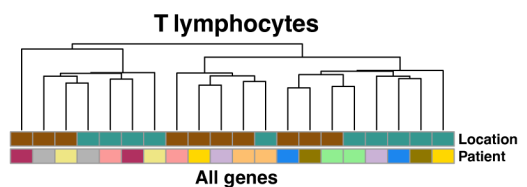
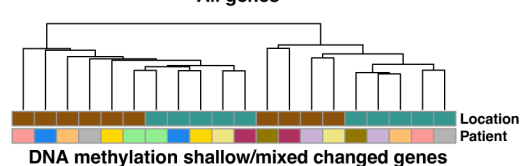
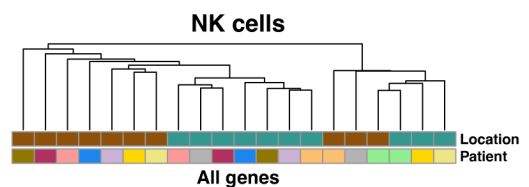
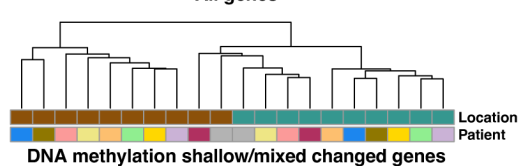
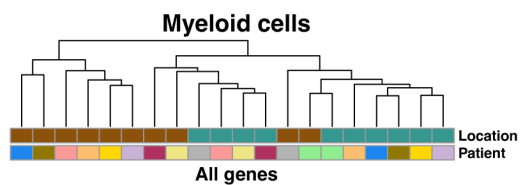
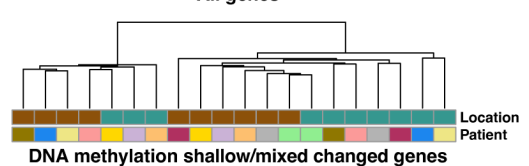
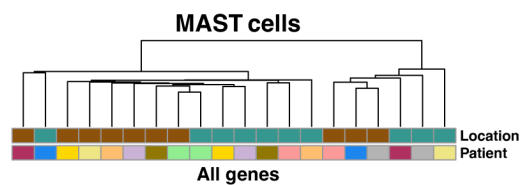
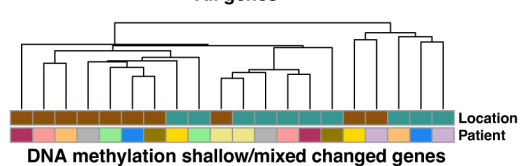
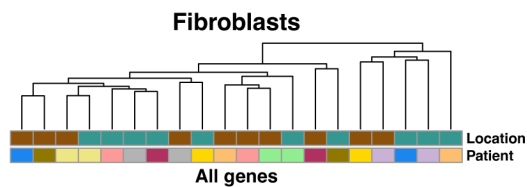
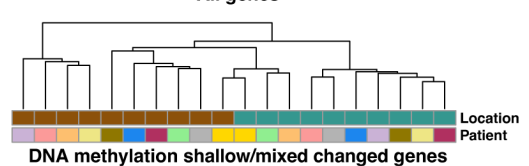
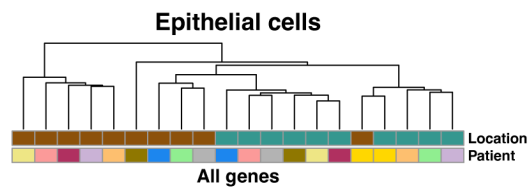
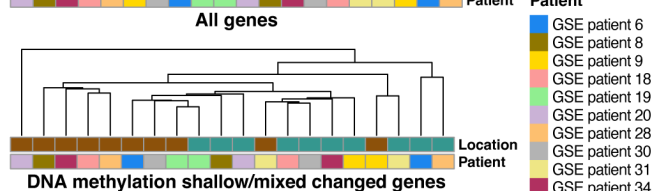
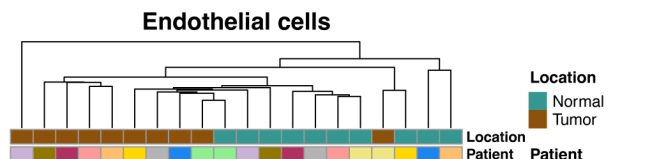
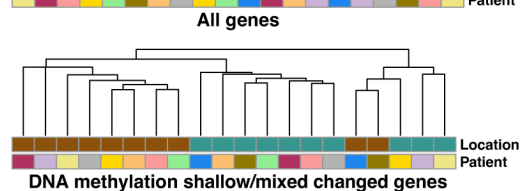
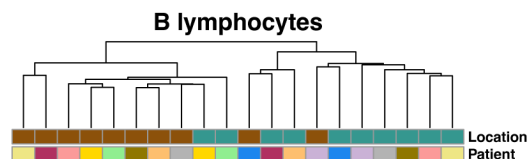
Appendix Figure S8. Single-cell RNA analysis of 80576 cells from 10 LUAD patients.

(A) UMAP plot of cells colored by major cell types. (B) UMAP plot of cells colored by cell subtypes. (C) Expression levels of *CDKN2A*, *NOTCH1*, *PDGFRA*, and *WNT7B* across different cell types in tumor samples (upper four panels) and normal samples (lower four panels). *FZD10* was excluded from the analysis due to low expression.



Appendix Figure S9. Impact of cell type exclusion of each patient on target gene log2FC.

Log₂ fold change of aggregated expression differences for target genes between tumor and normal tissues across patients after excluding specific cell types. Pseudo-bulk expression profiles were generated by aggregating single-cell RNA-seq data from different cell types within each patient sample. For each patient, log₂ fold changes between tumor and normal tissues were calculated based on the full dataset (“None”) and after systematically removing one cell type at a time: B lymphocytes, endothelial cells, epithelial cells, fibroblasts, myeloid cells, and T lymphocytes. Each line represents the resulting fold-change profile after the exclusion of a specific cell type. Variability across cell-type exclusions reflects the contribution of individual cell populations to observed expression differences of the target genes.



Appendix Figure S10. Clustering of gene expression profiles in different cell types.

The gene expression patterns of various cell types in tumor and normal samples from different patients are clustered. Each group is a cell type. The upper panel is the situation of all expressed genes, and the lower panel is the expression spectrum clustering of genes with shallow or mixed changing regions.

Appendix Methods

Pipeline of DNA methylation changing trend statistics

Here we explain in more detail the screening process and various standards for the changing trend sites in our study, combined with more examples, in the hope that readers can better understand and reproduce the results, and recognize the rigor of the presented data.

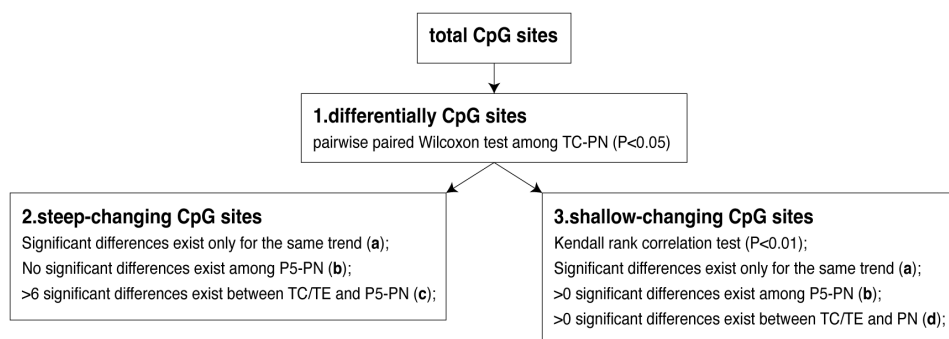


Figure 1

As shown above, our overall screening process can be divided into three steps, including extracting sites with methylation differences from the total CpG sites and performing some feature statistics for these sites in the main text. Then, the steep- and shallow-changing sites were screened among the remaining sites according to different inter-position differences.

Compare between positions and create significant matrices

First, we need to figure out the differences between different sampling positions of each site. We grouped each CpG site by sample location and compared methylation between groups pairwise.

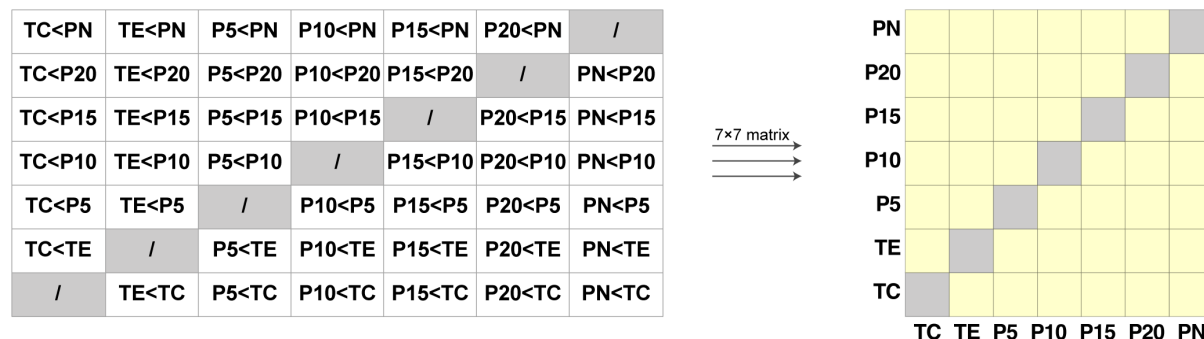


Figure 2

The paired one-tailed Wilcoxon test was used to count the significance with a $P < 0.05$ threshold, and 42 comparisons were done for each CpG site (as Fig.2 shows). From the results of the comparison between groups, a 7×7 logical matrix can be formed as the significant matrix, on which each position corresponds to whether the difference between the two groups is significant.

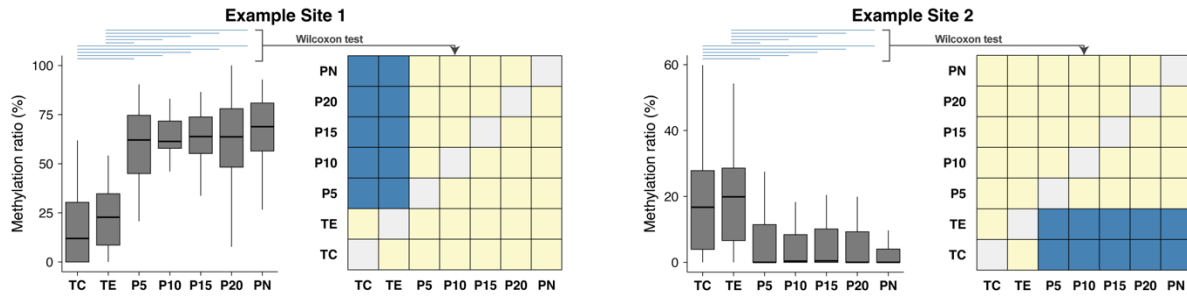


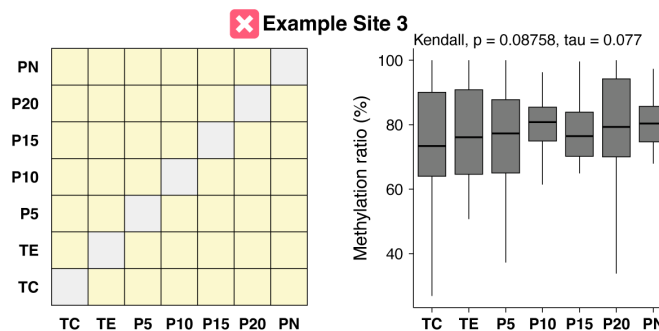
Figure 3

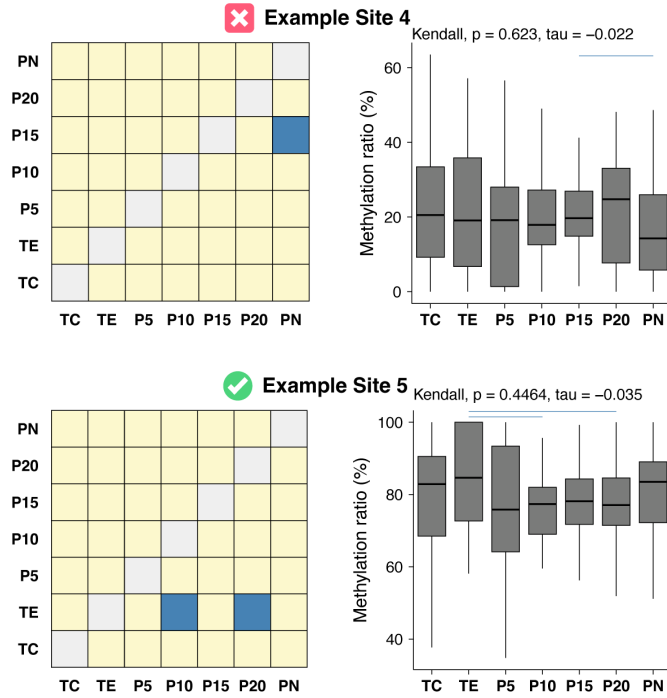
For example, in Fig.3, methylation of Example 1 on TC and TE were significantly less than on P5 to PN, while methylation of Example 2 on TC and TE were significantly higher than on P5 to PN, respectively.

From total CpG sites to differentially-methylated sites

For all CpG sites, many did not have any significant difference in methylation across different locations, and the observation of different characteristics will be affected when these sites are retained. To better extract the location characteristics of the differences, we only retained the CpG sites with at least two significant differences for subsequent analysis, and finally, a total of 613,724 CpG sites were obtained with significance between at least two comparisons.

Examples:





For example, in Fig.4, there was only 0 and 1 significant difference between the positions of Example 3 and Example 4, respectively, while Example 5 had significance on $P10 < TE$ and $P20 < TE$. In these three sites, we would keep Example Site 5 for the next part.

From differentially-methylated sites to steep-changing sites

When the screen for steep-changing sites, we first required the differences must occur on the same side, to exclude some sites with fluctuating methylation changes by position order (area A marked in Fig.4A). The steep-changing sites should mainly reflect the difference between tumor tissue and non-tumor tissue, so we required there should be no difference among P5-PN (area B marked in Fig.4B). At the same time, we require sites have no less than 6 significant differences between TC/TE and P5-PN to conform to the trend of steep changes (area C marked in Fig.4C). In the end, we got sites with the steep-changing trend.

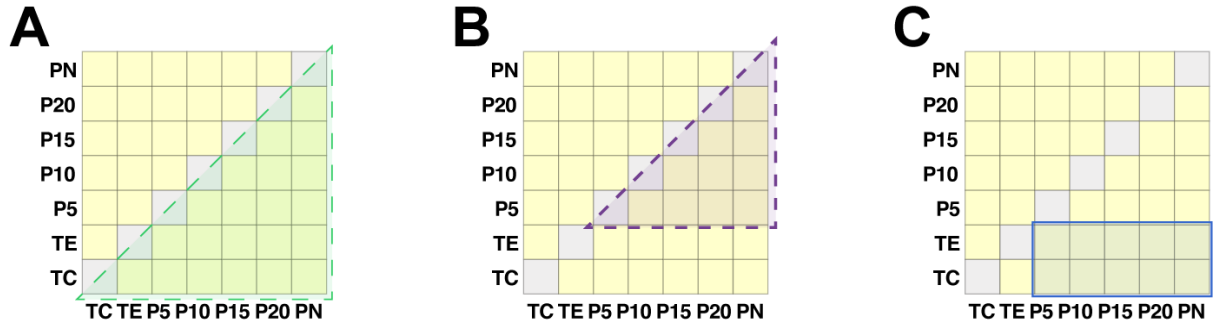
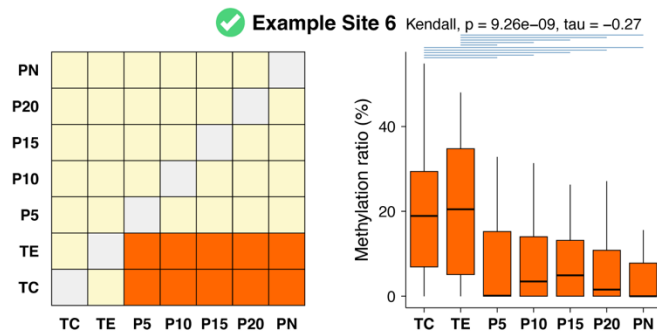
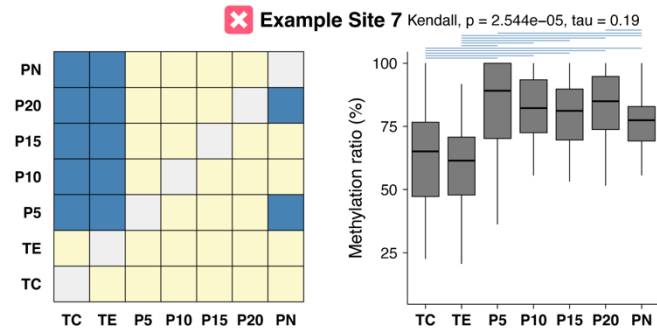


Figure 4

Examples:

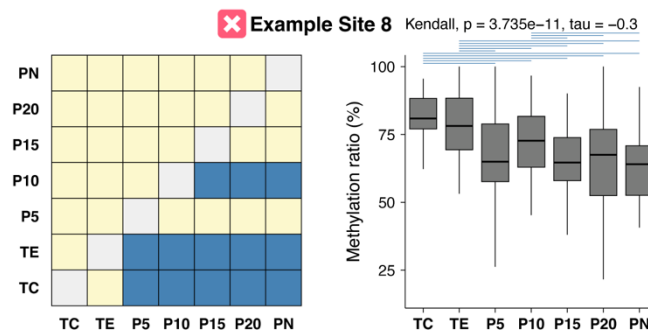


In Example 6, methylations on P5-PN were significantly less than on TC and TE, respectively, counting for 10 significant differences in area C. Besides, all significant differences occurred on the same side and no significance occurred in area B. So, we take this site as a steep-changing CpG site.

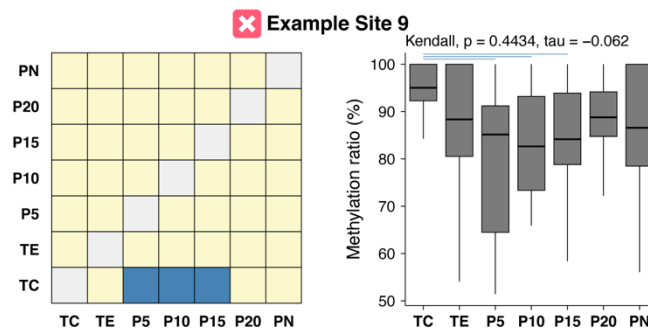


In Example 7, there were significances on both sides, which didn't meet the requirement. Although there are enough differences in area C, indicating methylation on TC and TE were

significantly different from P5 to PN, it is not difficult to see fluctuations in methylation levels between PN and P20 and between PN and P5, inconsistent with the overall trend.



In Example 8, there were significances in area B, which didn't meet the requirement. Due to the differences between non-tumor samples, it is not difficult to see that the methylation level in the adjacent samples is lower than that of the tumor but higher than that of distant normal tissues. We think this methylation change trend is more similar to shallow-changing, which describes gradual changes.



In Example 9, there were not enough significances in area C.

From differentially-methylated sites to shallow-changing sites

When it comes to shallow-changing sites, in the order of TC, TE, P5, P10, P15, P20, and PN, we performed perform ranking-based non-parametric tests, calculated Kendall's rank correlation coefficient of methylation at each significant difference site, and screened with $P < 0.01$. Same as steep-changing sites, we screened sites with all significant differences on the same side (area A marked in Fig.5A). For shallow-changing sites, significant changes should be seen between non-

tumor tissues, so we required at least one difference happened among P5-PN (area B marked in Fig.5B). Considering that the shallow-changing sites gradually changed with the distance, we did not require that there were huge differences between TC/TE and P5-PN but only need to ensure that there was difference between TC/TE and the farthest PN (area D marked in Fig.5C). In the end, we got sites with the steep-changing trend.

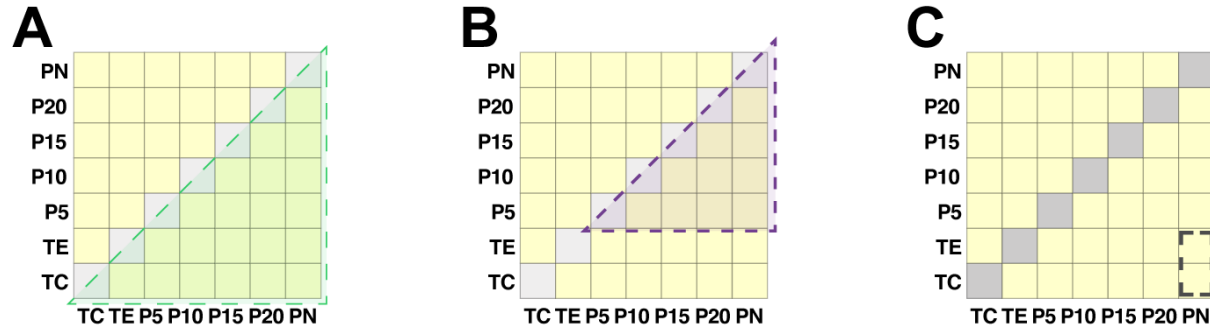
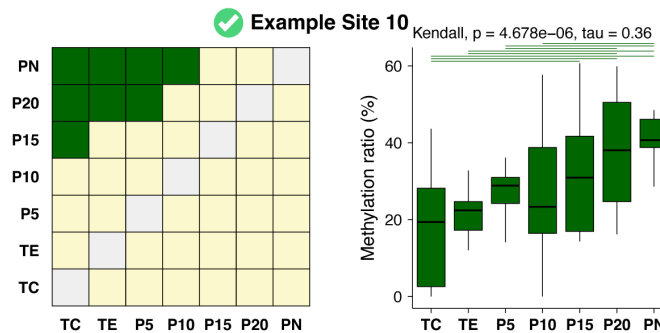
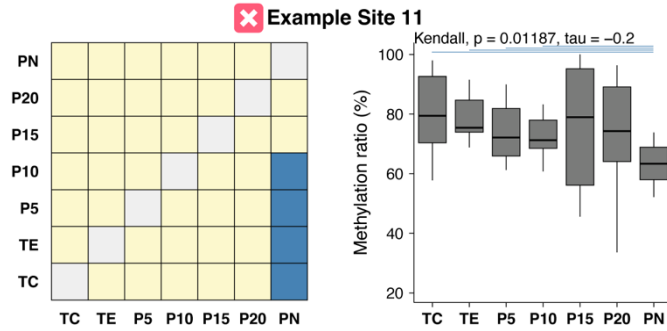


Figure 5

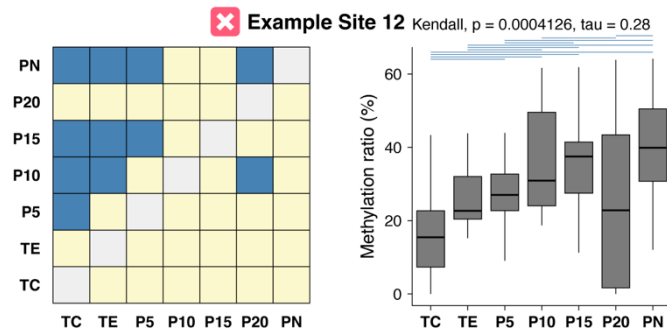
Examples:



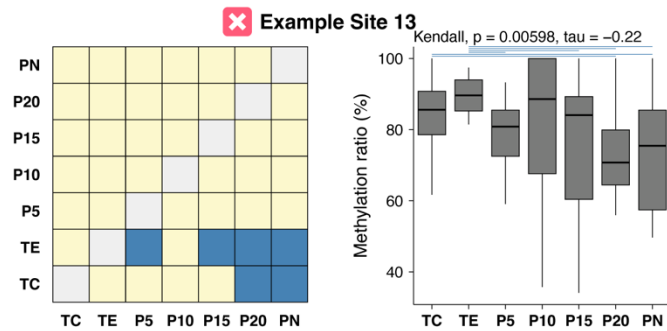
Example 10 is a shallow-changing site. It had a P -value < 0.01 in Kendall's correlation test. Methylation on TC was significantly less than on P15 to PN, TE and P5 less than P20 and PN, and P10 less than PN. The difference pattern of the site met the requirement above. So, we take this site as a shallow-changing CpG site.



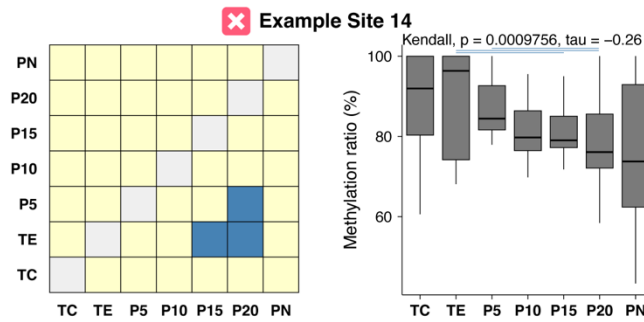
In Example 11, the P-value of the site in Kendall's correlation test is higher than 0.01. Although the rest of the features meet our requirements, it was excluded.



In Example 12, there were differences on both sides, which might reflect potential fluctuations in methylation, and it was excluded.



In Example 13, there were no significant changes between non-tumor tissues, so this site was excluded.



In Example 14, methylation significantly decreased with distance, and there was a significant difference between P5 and P20. However, such points were excluded due to the absence of significant differences between tumor (TC, TE) and distant normal tissue (PN).